



Rapid detection of bacterial infection and viability assessment with high specificity and sensitivity using Raman microspectroscopy

Srividya Kumar¹ · Renu Gopinathan² · Goutam Kumar Chandra^{1,3} · Siva Umamathy^{1,4} · Deepak Kumar Saini^{2,5,6}

Received: 14 November 2019 / Revised: 5 January 2020 / Accepted: 30 January 2020 / Published online: 19 February 2020
© Springer-Verlag GmbH Germany, part of Springer Nature 2020

Abstract

Infectious diseases caused by bacteria still pose major diagnostic challenges in spite of the availability of various molecular approaches. Irrespective of the type of infection, rapid identification of the causative pathogen with a high degree of sensitivity and specificity is essential for initiating appropriate treatment. While existing methods like PCR possess high sensitivity, they are incapable of identifying the viability status of the pathogen and those which can, like culturing, are inherently slow. To overcome these limitations, we developed a diagnostic platform based on Raman microspectroscopy, capable of detecting biochemical signatures from a single bacterium for identification as well as viability assessment. The study also establishes a decontamination protocol for handling live pathogenic bacteria which does not affect identification and viability testing, showing applicability in the analysis of sputum samples containing pathogenic mycobacterial strains. The minimal sample processing along with multivariate analysis of spectroscopic signatures provides an interface for automatic classification, allowing the prediction of unknown samples by mapping signatures onto available datasets. Also, the novelty of the current work is the demonstration of simultaneous identification and viability assessment at a single bacterial level for pathogenic bacteria.

Keywords *Mycobacterium tuberculosis* · Diagnosis · Raman spectroscopy · Viability assessment

Electronic supplementary material The online version of this article (<https://doi.org/10.1007/s00216-020-02474-2>) contains supplementary material, which is available to authorized users.

✉ Siva Umamathy
umamathy@iisc.ac.in

✉ Deepak Kumar Saini
deepaksaini@iisc.ac.in

¹ Department of Inorganic and Physical Chemistry, Indian Institute of Science, Bangalore 560012, India

² Department of Molecular Reproduction, Development and Genetics, Indian Institute of Science, Bangalore 560012, India

³ Department of Physics, NIT Calicut, Calicut, Kerala 673601, India

⁴ Department of Instrumentation and Applied Physics, Indian Institute of Science, Bangalore 560012, India

⁵ Centre for Biosystems Science and Engineering, Indian Institute of Science, Bangalore 560012, India

⁶ Centre for Infectious Diseases Research, Indian Institute of Science, Bangalore 560012, India

Introduction

Rapid and accurate diagnosis of the causative organism plays a vital role in infectious disease epidemiology [1]; however, one of the fundamental challenges in this area lies in the accurate identification of the causative agent. The need is to have a method that not only identifies pathogen signatures accurately but also provides the viability status of the pathogen, which is imperative for understanding the pathogen's response to therapy and for deciding on a future therapeutic regimen.

Conventional diagnostic techniques like microbial staining or culturing of the pathogen from clinical samples remain the gold standard for detection of many pathogens including *Mycobacterium tuberculosis*, the causative organism of tuberculosis (TB). Although these approaches are relatively inexpensive and simple, the major disadvantage is that they are contingent on the bacterial load in the sample and the time taken for identification may vary from days to weeks depending on the bacteria. For example, smear culturing requires at least 10^4 bacilli per milliliter of sputum sample [2]. Furthermore, only live culturable bacteria can be detected using standard growth-based techniques. Viable but non-culturable bacteria (VBNCs) which are metabolically viable

but not culturable due to the lack of knowledge of their preferred growth conditions or due to dormancy successfully elude culturing tests, thereby resulting in false negatives and making these techniques non-adaptable for point-of-care diagnostics. Recent advances in molecular biology have facilitated the development of polymerase chain reaction (PCR) [3, 4] and other nucleic acid-based amplification techniques such as line amplification assay [5] and serology-based assays as methods of choice for accurate and rapid prognosis without the need for cultivation of the pathogen [6]. However, they are fraught with either low sensitivity due to a paucity of organisms in the sample or they provide false-positive results due to contamination of the sample with environmental bacteria [2]. A further complication is introduced by the fact that DNA can be isolated from both live and dead organisms and thus cannot confirm the presence of live pathogens. Moreover, assays which rely on detecting circulating antibodies against pathogen antigens have the major limitation of cross reactivity of antibodies to antigens from closely related bacterial species which can generate false-positive results [3]. Furthermore, these assays do not provide information regarding the resistance to the antimicrobial agents unless they have standard mutations [7–9]. Skill intensiveness and multistep sample processing designs of existing diagnostic technologies also require trained manpower, which may be a limitation at the point of care in low-income countries.

Therefore, a technique which can specifically analyze biochemical signatures of bacteria and distinguish live from dead populations can aid in addressing these requirements. One of the ways to fingerprint the complete biochemical composition of an organism is to use vibrational microspectroscopic techniques, namely infrared and Raman spectroscopy [10–14]. These techniques can capture bond-specific vibrations from biochemical constituents of the cell. They can also achieve spatial resolution for single bacterial or single colony biochemical fingerprinting using a microscope along with a spectrograph. Infrared and Raman microspectroscopy along with multivariate analysis has been employed previously in strain-specific identification of bulk bacterial samples [15–17]. Due to the challenges of infrared optics, analysis of a single bacterium is arduous. In contrast, Raman microspectroscopy which primarily operates in the visible spectrum can attain high spatial resolution with the use of high magnification and high numerical aperture (NA) objectives.

In this study, we have demonstrated simultaneous identification and viability assessment of bacteria using tuberculosis (TB)-causing bacteria, *Mycobacterium tuberculosis*, as the model system. Towards this, primarily, a background-free substrate is developed for Raman analysis of a single bacterium. Secondly, an appropriate fixative agent suitable for Raman analysis of bacteria, which makes them non-viable without affecting their biochemical signatures, is described. Further, viability assessment was demonstrated for bacteria

spiked in artificial sputum. Finally, a proof of concept showing a concurrent methodology for species identification and viability assessment using Raman microspectroscopy is presented. Though there are reports on single bacterial identification of tuberculosis, the novelty of the work is the concurrent approach for viability assessment for the pathogenic bacteria. Furthermore, the method can be scaled to any number and type of bacteria.

Materials and methods

Description of protocols regarding bacterial strains and culture, fixation, drug and artificial sputum treatment of bacteria, and their biological viability assessment are given in the [Electronic Supplementary Material](#) (ESM).

Substrate fabrication Fig. S1 (see ESM) depicts briefly the protocol utilized for fabricating the substrate. 100 p-type silicon (Si) wafer was cleaned to remove any oxides or ions using the standard RCA cleaning procedure, followed by deposition of a layer of 200 nm aluminum using either thermal evaporation or by sputter coating. The deposited aluminum was annealed at 400 °C in a N₂ atmosphere for 15 min. These substrates were stored inside a desiccator until use. The bacteria were dry-casted on the substrate. Further, the substrate was mounted on an aluminum holder which facilitates mounting to the microscope stage.

Processing of bacterial samples for Raman spectroscopy The cells were pelleted and washed with 1 ml of deionized water. Washing was repeated twice for cultured bacteria and 5 times for cells obtained from the sputum. After the last wash, the pellet was resuspended in MilliQ water and from that 1.5 Microlitre was cast on the fabricated Raman substrate and dried at room temperature before spectroscopic measurements.

Raman microspectroscopy analysis Raman measurements were performed using a Renishaw InVia Raman microspectroscope. Initial experiments on quartz substrate were performed using 514 nm laser whose results are shown in Fig. S2 (see ESM). Further experiments were performed using the 633 nm on an upright microscope with a laser power of ~10 mW. The Raman spectra of individual bacteria were collected using a ×100 dry objective (0.8 NA). The same objective was used to collect the backscattered light from the sample. The scattered radiation was passed through a notch filter, focused onto a monochromator with 1200 lines/mm grating, and detected using a Peltier cooled CCD camera (256 × 1048 pixels sensor). For spectroscopic evaluation of the lower wavenumber region (500–1900 cm⁻¹), the bacteria were exposed for 15 s and the spectra were accumulated 5 times to get a good SNR. For the higher region (2800–

3000 cm^{-1}), 10 s exposure and 3 accumulations were done. Each experiment has three biological replicates, and each biological replicate had a minimum of two technical replicates. A minimum of fifty bacteria were sampled from each biological replicate. In total, more than 2500 spectra were used for simultaneous identification and viability assessment. Further, for imaging experiments, more than a thousand spectra were collected which depends on the size of the imaging area. After data collection, the spectra were subjected to pre-processing including cosmic ray removal, multipoint base line correction, Savitzky-Golay smoothing, and vector normalization using Renishaw wire 4.2, OriginPro 8.5 and Unscrambler 10 software. Unlike univariate analysis where few wavenumbers are picked for analysis, all the wavenumbers of a spectrum are employed for the analysis. IBM SPSS 17.0 for canonical discriminant analysis (CDA) and Unscrambler 10 was employed for principal component-linear discriminant analysis (PC-LDA) in which predictions of unknown samples were performed. The CDA uses the leave-one-out-cross validation (LOOCV) method to validate the model. In this method, one sample is kept out as test data and the rest of the sample is employed to build the training dataset. Then the test data is fed to check whether it is being correctly identified in their respective class/cluster/group. Likewise, each sample is kept out of the training set and evaluated. The outcome of these iterative processes is a measure called accuracy which tells the robustness of the model built. Accuracy is directly dependent on the correct clustering of the test data to its appropriate group.

Results

Towards developing a rapid non-invasive diagnostic tool for the identification of bacterial infections, we focused on diagnosing tuberculosis through Raman signatures. Tuberculosis (TB) was taken as the case study to demonstrate the identification potential, effect of decontamination, and viability assessment using Raman microspectroscopy. This was primarily because TB accounts for the maximum number of deaths caused by a single infectious agent and the high mortality is due mainly to improper diagnosis, long therapeutic regimens, and poor patient compliance. As Raman scattering is a weak process, to achieve a good signal-to-noise ratio (SNR) from a single bacterium, we first developed a background-free substrate (Fig. 1a). Further, we deduced appropriate Raman measurement parameters to record spectra from single bacteria rapidly with high SNR (Fig. 1b). We typed several *Mycobacterium* species belonging to the *M. tuberculosis* complex (MTC) and non-tuberculous *Mycobacteria* (NTM) group alongside many common bacteria like *Escherichia coli*, *Bacillus subtilis*, *Klebsiella pneumoniae*, etc. to build a spectroscopic database based on Raman spectral signatures (Fig. 1c). To extend the protocol to pathogenic bacteria, we

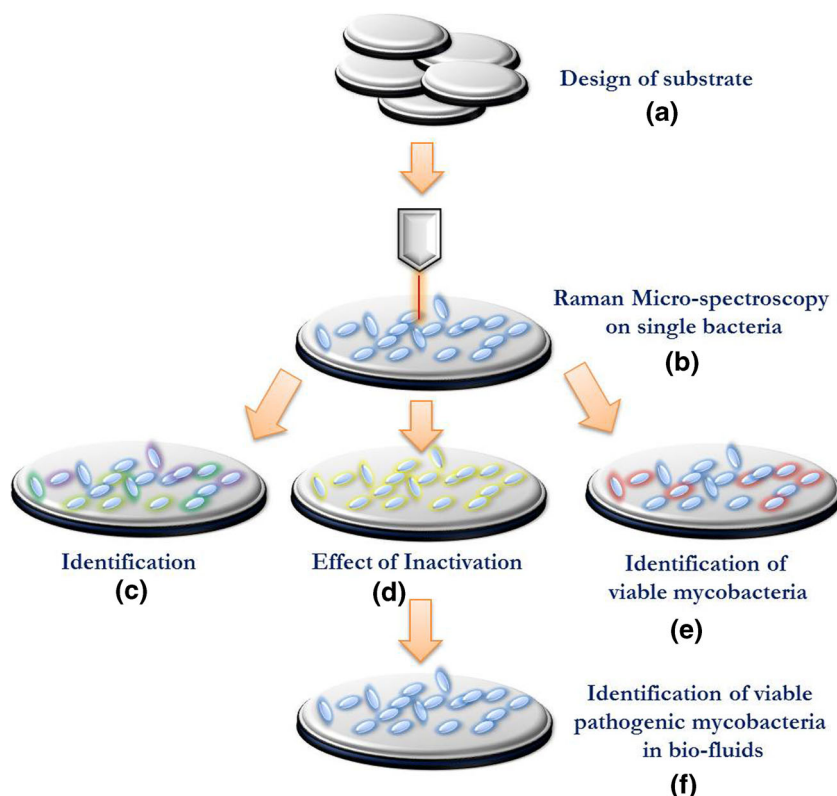
identified suitable chemical inactivation methods for *Mycobacteria* which would have a minimal consequence on Raman spectra (Fig. 1d). In addition, we were also able to generate spectral signatures which can differentiate dead bacteria from live, by generating spectra from mycobacteria cells treated with first-line drugs as against untreated live cells (Fig. 1e), thereby addressing one of the long-standing needs of clinical microbiology, i.e., to discriminate between live and dead bacteria in a clinical-like sample (Fig. 1f). Overall, our study reports a reliable, rapid, and non-invasive diagnostic tool that can be adapted as a point-of-care diagnostic testing in clinics, especially for tuberculosis. Our approach is amenable to the identification of live and dead bacteria, and to the best of our knowledge, this is the only technique which can rapidly identify bacteria and assess their viability status as well.

Identification of appropriate substrate and laser wavelength for Raman analysis of bacterial populations

Substrate and choice of wavelength play a major role for Raman scattering-based analysis of biological specimens as they affect the signal-to-noise ratio. Quartz substrates are widely employed in Raman spectroscopy but have a strong background contribution in the fingerprint region (800 to 1800 cm^{-1}) as shown in Fig. S2a (see ESM). Kerr et al. have provided a detailed account of these issues and have identified substrates which suit mammalian cells [18]. Several background-free substrates like CaF_2 , MgF_2 , etc. are widely used in Raman spectroscopy of biological samples like mammalian cells, tissue, and bulk bacteria. However, these substrates do add background while employing for single bacterial analysis as the volume that we are measuring is very small compared to other biological samples mentioned before. So, we developed a substrate for Raman imaging of a single bacterium. A detailed account of the steps we have taken to develop a substrate is given in the ESM (Fig. S1). This substrate was similar to aluminum-coated slides used previously for identification of environmental bacteria [19].

Raman spectra from five different species of bacteria, namely *E. coli*, *B. subtilis*, *K. pneumoniae*, *Mycobacterium smegmatis*, and *Mycobacterium bovis*, were recorded after drop casting on the in-house fabricated substrate with both 514 nm and 633 nm excitation light sources as shown in Fig. 2. The sensitivity obtained from PC-LDA of Raman spectra with 514 nm and 633 nm was 100% and 99.63% respectively. Both excitation sources provided high accuracy on prediction using PC-LDA which is seen in the confusion matrix given in Table S1 (see ESM). The confusion matrix is a way to represent the reliability of an experiment, wherein inaccurate or less specific readouts will result in higher values in wrongly classified columns. Though both wavelength sources provided high accuracy, further experiments were performed with a 633-nm

Fig. 1 Overview of the study. The steps involved in developing a Raman-based single bacterial identification and viability assay are depicted. The process starts from design of appropriate substrate (a) which is free of background signal and which facilitates spotting of single bacteria. Following the design of substrates, optimal Raman spectroscopic measurement parameters were framed for further analysis (b). The primary step is to classify a single bacterium based on the Raman spectra (c), followed by investigating the effect of fixatives (d) and antibiotics (e) that are used to eradicate mycobacterium. Finally, the methodology to identify viable pathogenic bacteria is used to establish the Raman-based viability assay to suit the clinical setting (f)



laser line because this wavelength shows considerably less phototoxicity and lower background fluorescence [20]. Utilization of this single bacterial Raman imaging platform, essential for mixed culture analysis, is described in detail in ESM (Fig. S3).

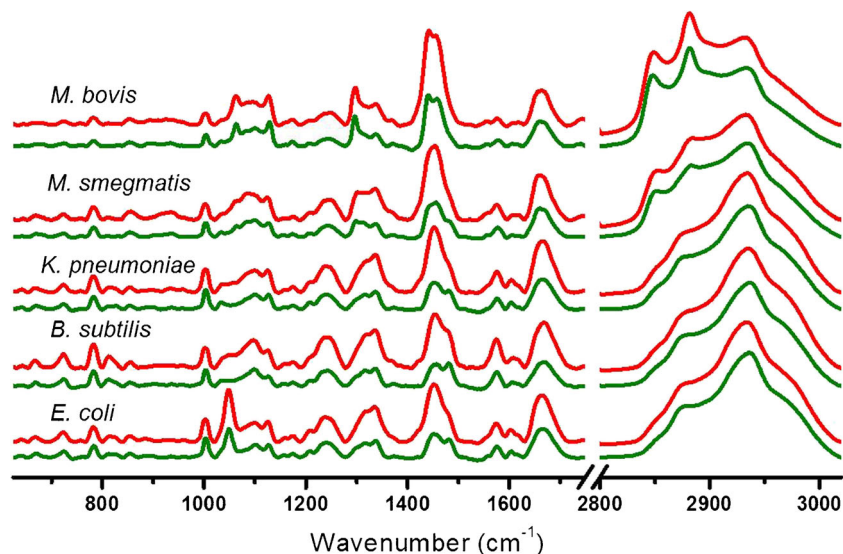
Optimization of sample processing for Raman spectroscopy for handling pathogenic bacteria

For bacterial samples obtained in clinical settings, decontamination is an essential requirement for the safe handling of

pathogenic samples. Decontamination is generally achieved by means of chemical treatment, but the choices are limited when it is desirable to retain the integrity of biological structures, preserving molecules, cells, and tissues at a specific stage for further composition analyses. This is classically obtained by fixation, which also protects the biological components from decay during harsh treatment protocols such as dehydration, washing, and staining.

Multiple approaches of sample fixation and decontamination have been utilized for different applications, and agents

Fig. 2 Average Raman spectra from a single bacterium from different species. The spectra were recorded using 514 nm (bottom green trace) and 633 nm (top red trace) lasers as excitation light sources. The samples were mounted as described in the “Materials and methods” section, and Raman signatures were collected as described. Representative spectra collected from a single bacterium are shown



such as ethanol, paraformaldehyde (PFA), and sodium azide (only to a limited degree) have been tested for Raman spectroscopy previously on various bacterial species [21]. However, both samples as well as downstream processing determine the right fixative and decontaminating agent. We tested various chemical agents to identify a suitable method for detoxification as well as for preserving the cellular integrity of bacterial samples. The efficacy of various agents was tested using *M. smegmatis* as a test bacterium on two specific parameters, (i) loss of cell viability and (ii) retention of Raman signatures. The morphology of *M. smegmatis* was unaltered for all the three selected agents (Fig. 3a and ESM Fig. S4), and the Raman spectra were recorded from live, untreated, and unfixed cells and compared with treated and fixed *M. smegmatis* (Fig. 3b). As evident from the spectra, there are no remarkable differences observed between the samples. Figure 3c depicts the difference spectra obtained when the average Raman spectra of unfixed bacteria were subtracted from the fixed ones. Post subtraction, the positive and negative values indicate the extent of changes that have occurred in a bacterium due to the

treatments. Among the three agents, PFA showed the least variation and glutaraldehyde treatment showed the most changes in the composition in comparison to the live samples. While sodium azide-treated cells showed minimal spectral changes, the viability assessment revealed that the bacteria were not dead after this treatment (Fig. 3a), thereby not meeting the integral requirement for further processing steps. Thus, PFA was selected as the fixative for processing *Mycobacterial* samples for Raman spectroscopy. Suitability of processing was further proved by CDA (Fig. 3d) wherein the PFA-fixed cells clustered close to the unfixed ones. The method was also suitable for recording the spectrum from the pathogenic *M. tuberculosis* (red curve in Fig. 3e). The spectra from fixed and decontaminated *M. tuberculosis* were comparable to that of *M. bovis*, a close but non-pathogenic relative which can be handled in BSL2 laboratory settings. The spectra also show that both the species have very similar chemical composition based on Raman analysis. Overall, we report the development of a complete workflow for Raman analysis of pathogenic bacterial species which does not interfere with their identification.

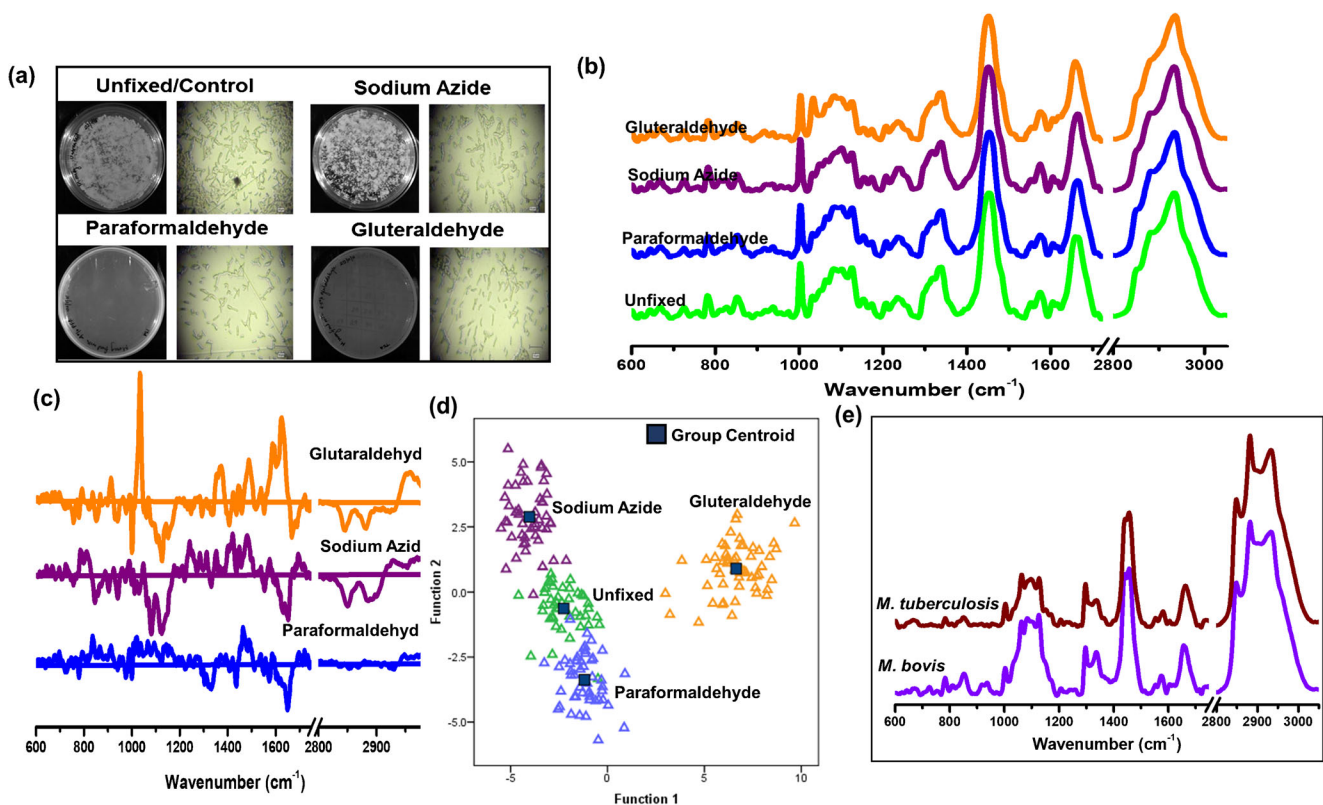


Fig. 3 Effect of various decontaminating agents on Raman analyses. **a** Viability assessment for various decontamination agents using a plate-based culturing assay and the white light image of treated *M. smegmatis* cells under $\times 100$ magnification to monitor any change in morphology (if any). **b** Average Raman spectra from *M. smegmatis* cells treated with

various agents utilized for eradicating them and their comparison with live cells. **c** Differences in Raman spectra of bacterium treated with various inactivating agents. Baseline spectra are from live bacteria. **d** CDA for live and fixed bacterial cells. **e** Comparison of spectra collected from fixed *M. tuberculosis* with that collected from fixed *M. bovis*

Development of a Raman-based viability assessment tool for bacterial cells

One of the main limitations of most microbial diagnostic tools such as PCR, ELISA, and so on is their inability to provide information about the viability of the sample. Culturing techniques, which can distinguish live from dead bacteria, are generally very slow and limit handling of biological samples to only approved laboratories (BSL2 and above). Towards investigating the applicability of Raman spectroscopy for overcoming these limitations, we approached the problem in two steps. First, to evaluate if the signatures of viability are retained even after fixation and, second, if Raman microspectroscopy can distinguish between live and dead bacterial cells (discussed in the next section).

Towards the first step, *M. smegmatis* cells were cultured in the presence or absence of various antibiotics, typically used for treating tuberculosis, viz. streptomycin, rifampicin, ethambutol, and isoniazid. The cells were treated either with each drug independently or with all together as done in the standard treatment course. The bacterial cells were treated with indicated doses for 24 h before Raman analysis, where effects on *M. smegmatis* are recorded.

As anticipated, in our experiments, we recorded complete cell death when all the four antibiotics were utilized together, but variable killing was recorded with individual antibiotics by culturing of the treated bacterial cells (Fig. 4a). Figure 4b shows average Raman spectra collected from treated and untreated *M. smegmatis*. Since each antibiotic targets different biological pathways, the average Raman spectra show changes in peak intensities, shape, and bandwidth for various spectra. While we did not characterize the specific chemical changes because of each antibiotic treatment, we focused on differences in signature to distinguish the live and the dead bacteria (obtained by four antibiotic treatments).

Viability analysis clearly showed that only the bacteria treated with the combination of the selected four antibiotics were completely killed. We tested our ability to discriminate live vs dead bacteria using CDA as shown in Fig. 4c. The LOOCV accuracy was 83.4%. Low sensitivity of viability assessment arises due to absence of segregation of clusters. At the level of single bacterial analysis, it is difficult to be sure that the sampled bacteria are affected by the antibiotic treatment. Many bacteria in the culture may be resistant to antibiotics or may grow with a low rate. For example, the signature of ethambutol-treated cells showed only an increase in carotenoid peaks and was similar for the most part to untreated or live cells. Moreover, only the combinatorial therapy which succeeded in killing all the cells clustered away from the live ones. In addition, the streptomycin-treated cells cluster with the dead bacteria and the centroids of both the cluster are located close to each other. Further, the Raman spectra of the streptomycin-treated cells alone and the combined treatment

of four antibiotics showed more comparable signatures. As evident from the plate growth effect, streptomycin was the strongest antibiotic, but by itself, it did not eradicate all the bacteria. Concomitant to this, Raman spectral analysis revealed that the bactericidal effect of streptomycin is higher compared to that of the other antibiotics and the treated bacteria grouped closer with the dead ones. The rifampicin-treated cells clustered between the live and the dead cells, and the centroid was closer to the dead cell cluster. The isoniazid-treated cells formed a completely different cluster equidistant to both live and dead clusters, perhaps on account of its completely different mechanism of action which needs activation by bacterial catalase and by itself can be used for treating latent bacteria. These findings provide a unique platform to typing bacterial cells from patients and identify which antibiotics they are responding to. This can be one experimental strategy which can be employed to identify drug resistance in bacterial cells.

Finally, while comparing the live, dead, and fixed bacteria, the CDA gave us a cross validation accuracy of 98% (Fig. 4d) and the three groups clustered separately. Although both fixation and killing of bacteria by antibiotics lead to loss of viability, the modes of action are different resulting in two different clusters, evident in Fig. 4d. Technically, fixed cells are dead, evident from the plate assay. Interestingly, paraformaldehyde treatment-mediated fixation allows retention of the biochemical signatures in the cells even though they differ from the live and the dead groups. If we consider fixed as dead, then Raman is able to identify different deactivating procedures. While fixation leads to immediate arrest of cellular processes by cross linking the cellular ingredients, the drug-induced killing is a slow process, in which cellular pathways are blocked and thus leading to degradation of intracellular macromolecules, followed by death, which is reflected in their biochemical signatures and composition. Further, we performed ratiometric analysis of few peaks to appreciate the differences between live, dead, and fixed *M. smegmatis* (ESM Fig. S5) [12]. The ratios 811/825 corresponding to RNA/protein and 2853/2932 corresponding to CH stretching vibrations did not show any significant changes while comparing the live, dead, and fixed *M. smegmatis*. The ratios 782/1003 (DNA/protein), 851/938 (protein/glycogen), 918/938 (both peaks correspond to glycogen), 1283/1258 (peaks under the amide III region), and 1519/1575 (carotenoids/DNA) showed minimum or non-significant differences while comparing the live and fixed *M. smegmatis* (compare green and blue bars). Conversely, only the ratio 1083/1125 corresponding to phosphates and glycogen showed significant differences between the live and fixed samples. However, while comparing the live and fixed with the dead, we could observe mostly significant differences (compare the green and blue bar with the red). Further, the ratio 1450/1659 corresponding to lipid/protein had significant difference while comparing the three against

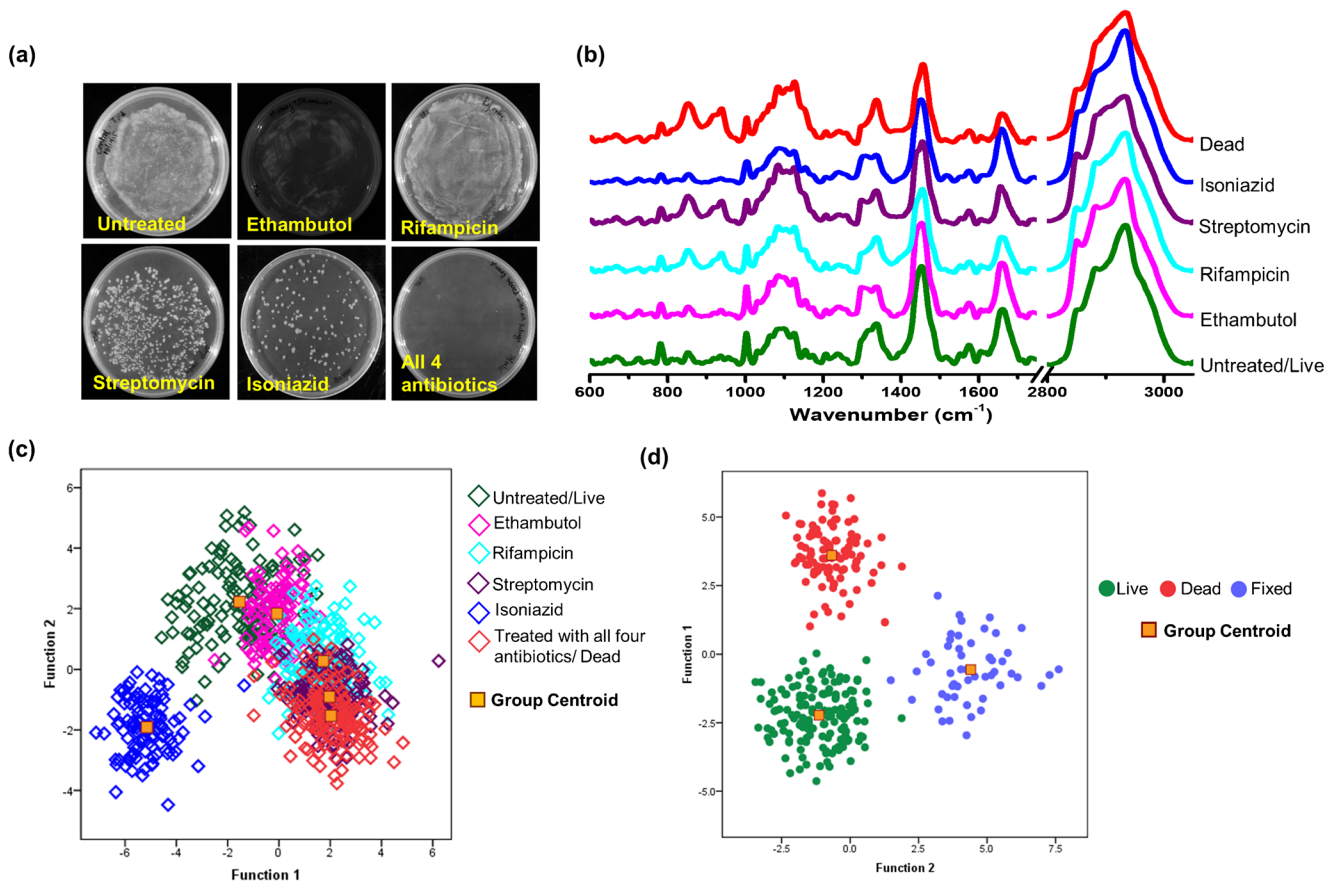


Fig. 4 Raman-based viability assessment for *M. smegmatis*. **a** Plate assay with various antibiotics or combination of antibiotics used to obtain bactericidal effects. Cells were treated with the filter sterilized antibiotics viz. isoniazid, ethambutol, rifampicin, and streptomycin with concentrations of 32 mg/ml, 42 mg/ml, 20 mg/ml, and 10 mg/ml

each other. Thus, most of the ratios remain similar for the live and fixed samples, thereby reinforcing the fact that the fixation through paraformaldehyde left the bacterium least affected whereas the dead which has undergone treatment with four antibiotics showed enormous differences. Overall, we report successful development and implementation of a rapid Raman-based viability assay for bacteria, essential for rapid diagnosis of bacteria present in clinical specimens.

Raman prediction and analysis of pathogenic bacterial samples in clinical material

Given that the ultimate objective of the study is to identify and characterize bacterial samples from clinical specimens, we next probed if the developed protocol based on Raman spectroscopy can be used for this. Towards this, mycobacterial cells were resuspended in artificial sputum media (ASM) and treated with the mucolytic agent N-acetyl cysteine (NaLC) and NaOH as per the standard Petroff's decontamination procedure. It is known that complex biological material like sputum, which is mainly mucous, can hinder the Raman

analysis; thus, it was essential to remove the same [22]. After this step, we fixed the sample with 4% PFA as described above and recorded the Raman spectra.

Figure 5a is the CDA plot of *M. smegmatis* in live and dead states after fixation. The LOOCV clustering of live, dead (obtained by treating with all four frontline drugs), and their fixed counterparts yielded an accuracy of 91.2%. LOOCV of discriminating the live and dead irrespective of fixation was 96.3% (confusion matrix shown in ESM Table S2). This served as a training dataset for the prediction of live and dead *M. smegmatis* samples spiked in artificial sputum.

ASM spiked bacteria fixed after NaLC treatment for removal of sputum were subjected to Raman analysis, and the spectra were predicted using PC-LDA on the training dataset. Figure 5b shows the outcome of this, where the first bar represents the prediction percentage of live (fixed) *M. smegmatis* spiked in ASM and 84% of the sample spectra were identified correctly as live and 16% were classified as dead.

The second bar represents the prediction percentage of dead (fixed) *M. smegmatis* spiked in ASM, and 82% were appropriately predicted as dead. Figure 5c shows the CDA

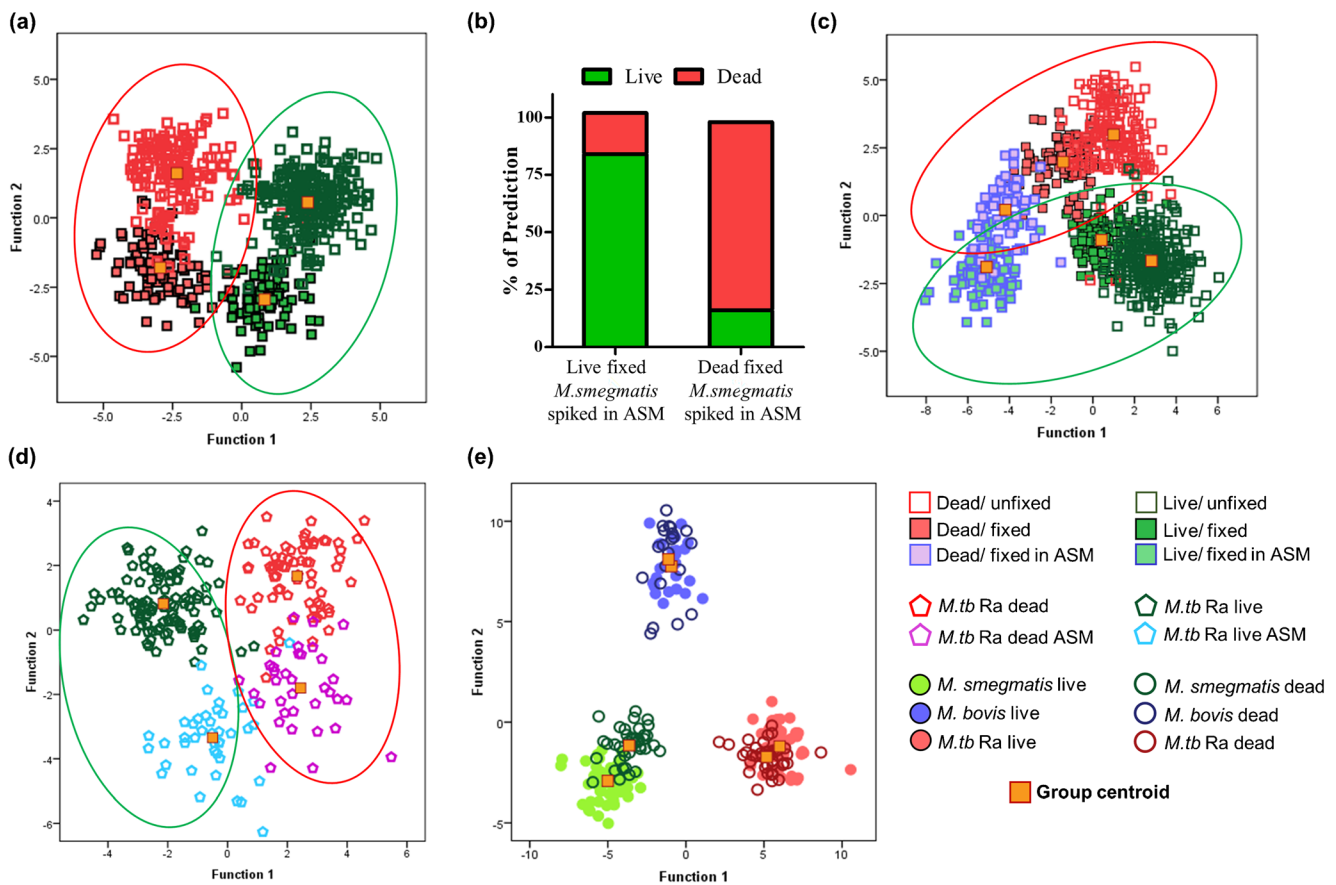


Fig. 5 Assessment of presence of viable pathogenic bacteria in biological fluids. **a** CDA of live fixed/unfixed and dead fixed/unfixed *M. smegmatis*. The cells were fixed using paraformaldehyde as per the protocol described in the “Materials and methods” section. To kill the bacteria, they were treated with all the four antibiotics as described in Fig. 4a. **b** Prediction analysis of various *M. smegmatis* cells (as indicated) spiked in ASM. **c** CDA of live and dead cells which are in fixed and unfixed state

and spiked in ASM. **d** CDA of the non-pathogenic strain of *M. tuberculosis* H37Ra and their live/dead classification after spiking in ASM. **e** CDA for species typing of pathogenic mycobacteria present in biological fluids (ASM) towards their identification and their viability assessment. The green oval corresponds to the live group and red corresponds to the dead group (irrespective of fixation or ASM treatment)

plot along with the sputum spiked samples, where the discriminant function 2 separates the live and dead with an accuracy of 93.7% (confusion matrix shown in ESM Table S2). The misclassifications observed between the live and the dead bacilli underscore the power of Raman spectroscopy to pick up natural variations in bacterial viability in a sample that has undergone no decontamination. Similarly, while sampling the dead, some bacteria would have escaped the complete effect of antibiotics and may have entered a viable but not culturable (VBNC) state and few of them are alive. Thus, the sensitivity of Raman spectroscopy at the single bacterial level surpasses all other existing methodologies.

A similar analysis was performed on pathogenic mycobacteria (fixed *M. tuberculosis* H37Ra). The CDA shows (Fig. 5d) an LOOCV accuracy of 97% in identifying the live and dead state of the bacteria post treatment and processing. The discrimination of live and dead irrespective of processing yielded an accuracy of 95% (confusion matrix shown in ESM Table S2). Overall, the workflow of developing a platform that facilitates species-wise identification of

bacterium regardless of their viability, fixation, and decontamination treatments is presented in Fig. 5e. The figure shows spectral analysis of *M. smegmatis*, *M. bovis*, and *M. tuberculosis* H37Ra in live as well as in dead states isolated from ASM. Following NaLC treatment and washes, the Raman spectra grouped into three broad clusters representing each species. Moreover, the centroids of live and dead bacteria (both fixed) for a given species always lie close to each other. Combined identification of the species and viability gave LOOCV accuracy of 94.6%, whereas the species identification irrespective of the viability gave LOOCV accuracy of 99.7%. This accuracy is like that of the initial identification shown in Table S1 (see ESM). CDA is a supervised classification model which demands declaration of groups in the dataset prior to classification. In Fig. 5e, the CDA model was built using a dataset whose species category is known prior to building the model. After the model was constructed, the sample points are represented with both the species identity and viability status to highlight that species identity is not lost in the process of testing the viability. However, for clinical samples, the spectra

were first processed through a model containing the species identity. Secondly, when viability is tested, it has the dataset of the particular species containing only its viability information. Thus, we present a method for bacterial species identification using Raman microspectroscopy wherein no effect of fixation, sputum components, and antibiotic treatment on the basic dataset is observed, but high sensitivity and specificity in sample identification are obtained.

Discussion

Raman-based bacterial identification has been reported previously, and the approach has also been used to identify and type mycobacterial strains in bulk [23–25]. Until 2003, identification of bacteria employed using Raman spectroscopy was mostly performed on bulk systems [26, 27]. From 2004, with the advent of confocal microscopy, high-magnification objectives and availability of highly sensitivity detectors, single bacterial identification and imaging through Raman have been explored [28, 29]. Studies have reported single bacterial identification for medically and environmentally relevant bacteria like anthrax [30], in urinary tract infection [31], in water pathogens [32, 33], in meat-associated pathogens [34], and in many other samples [16, 35–37] using multivariate analysis techniques. Raman spectroscopy along with supervised multivariate analysis techniques like support vector machine (SVM) has also been employed to identify TB pathogens, but no studies has reported use of Raman for identification and viability assessment [38]. In our study, in addition to the

identification of *M. tuberculosis*, we have studied the fixation effects as well as assessed the viability status of the microorganism. Further, the effect of antibiotics on bacteria, quantifying the MIC and the effect of different growth conditions have also been investigated [11, 39–43]. Apart from normal Raman studies, surface-enhanced Raman spectroscopy (SERS) which has enhanced sensitivity has also been employed for the identification of bulk and single bacteria including mycobacterial species and mycolates [44–49]. Investigations into antibiotic effects and the identification of antibiotic-resistant bacterial species have also been probed by SERS [50, 51]. Similarly, intracellular mycobacterial and staphylococcus species were identified and imaged inside the host cell using Raman microscopy [52, 53]. Fluorescence and SERS have been employed to test the viability of *Bacillus* and *E. coli* respectively [54, 55]. The effects of several fixation methods have been investigated on various bacterial species using Raman spectroscopy [21, 25, 56]. Overall, it is evident that the responses of bacteria to different treatments vary and consequently Raman spectra also vary. However, a unified approach for detection, inactivation, and viability assessment for a specific species of bacteria is yet to be explored as a protocol which, in future, can be applied to all bacterial species.

The current study presents a comprehensive and robust workflow for a Raman spectroscopy-based platform for bacterial identification and viability assessment at the single-cell level, which does not involve extensive sample processing. The study presents a design which overcomes the sensitivity and specificity limitations of microbiological procedures which are currently employed for strain identification and typing. Given that it is

Table 1 Comparison of features of the Raman-based diagnostic tool with the existing techniques

Parameters	Raman-based technique	Existing techniques
Sample processing	Only decontamination/fixation	Involves labor-intensive and time-consuming steps, either for extraction or for growth
Specificity	Raman spectrum reflects biochemical composition of a bacterium which is unique for each species. Even unknown bacteria can be classified to their closest related group. The limitation is defined only by the available database.	Though PCR serves as a gold standard for strain confirmation for low bacterial loads, prior information on conserved regions is required. Only the presence or absence of a particular strain whose primers are known can be identified irrespective of their viability status.
Sensitivity	Sample with any bacterial load is acceptable. With the use of high spatial resolution, a single bacterium can also be analyzed.	Many techniques utilize bacterial culturing from a clinical sample to increase their number for downstream analysis. PCR can potentially detect single bacteria.
Automation/simplicity	Needs minimum processing, only at the stages of decontamination, fixation, and casting.	Require extensive processing and handling. Errors or mishandling of sample scan lead to false negatives.
Running Cost	As it does not use any expensive chemicals, the running cost per sample is low. Although the spectrometer cost could be high, it would be a one-time infrastructure investment and not expected to have any recurrent cost component.	Running cost for PCR, microbiological, and other ELISA-based techniques on a per sample basis is high, as it requires expensive chemicals.
Speed	Maximum ~2 h after the sample is received	Ranges from 3 to 10 h for PCR and up to 21 days for culturing for TB identification
Expandability	As it detects the biochemical composition, the technique can be extended to understand treatment prognosis and their effect on the bacterium.	Culture tests and susceptibility analysis help frame the appropriate treatment regimen. Bio-molecular profiling is done by extraction of every component.

critical to know the viability status of the bacterial cells which are found in the biological samples, primarily to formulate appropriate therapy, the technique of choice for this purpose is still culturing, either in liquid in the form of growth indicator tubes or on solid medium; it can be a limitation in a sample where bacteria are viable but not culturable (VBNCs), a major impediment in microbiological assessment platforms worldwide [57]. This issue has been very difficult to surmount, and we present here an approach that can do so.

To summarize, we have (i) established Raman microspectroscopy as a sensitive and specific technique for the identification of various bacteria of MTC and NTM clades, (ii) demonstrated the ease of handling and processing of patient samples without changing any existing microbial typing protocols, (iii) demonstrated the ability of this technique to identify mycobacterial and other strains in artificial sputum, (iv) optimized the sample processing protocol for handling pathogenic bacteria, (v) proven the suitability of assessment of bacterial viability status at the single-cell level, and (vi) presented a facile platform for POC diagnostics.

With our protocol, we were able to successfully differentiate dead cells from the viable ones with a sensitivity of 98%, and even there we speculate the reduction in sensitivity could be due to the presence of VBNCs which otherwise are classified as dead, but Raman spectroscopy can potentially identify them. This finding is open to additional investigation and needs further characterization for various types of VBNCs, an area where conventional characterization tools have failed.

Finally, we present a feature comparison table for a Raman-based diagnostic tool for infectious diseases vis-à-vis the techniques currently in use like staining, culturing, and molecular tools (Table 1). While Raman spectroscopy is still in its infancy, we believe that it has the potential to develop into a one-step diagnostic tool capable of performing multiple analyses from a single sample, enabling early point-of-care diagnosis and prognosis tool of the disease followed by suitable antimicrobial therapy.

Acknowledgments S. Kumar acknowledges DST for INSPIRE fellowship. S. Umamathy acknowledges the Department of Science and Technology (DST Grant No. SR/S2/JCB-52/2009) and the Department of Biotechnology (Grant No. BT/01/CEIB/09/IV/05), Government of India, for financial support. S. Umamathy is a J. C. Bose Fellow of the Department of Science and Technology. D.K. Saini acknowledges the Department of Biotechnology (DBT Grant No. BT/PR3260/BRB/10/967/2011; BT/PR17357/MED/29/1019/2016), Government of India; DST-FIST [SR/FST/LS11-036/2014(C)], UGC-SAP [F.4.13/2018/DRS-III (SAP-II)], and DBT-IISc Partnership Program Phase-II (BT/PR27952-INF/22/212/2018) for infrastructure and financial support and Infosys Foundation for financial support.

Compliance with ethical standards

Conflict of interest The authors declare that they have no conflicts of interest.

References

- Walzl G, McNerney R, du Plessis N, Bates M, McHugh TD, Chegou NN, et al. Tuberculosis: advances and challenges in development of new diagnostics and biomarkers. *Lancet Infect Dis*. 2018;18(7):e199–210.
- Tiwari RP, Hattikudur NS, Bharmal RN, Kartikeyan S, Deshmukh NM, Bisen PS. Modern approaches to a rapid diagnosis of tuberculosis: promises and challenges ahead. *Tuberculosis (Edinb)*. 2007;87(3):193–201.
- Mothershed EA, Whitney AM. Nucleic acid-based methods for the detection of bacterial pathogens: present and future considerations for the clinical laboratory. *Clin Chim Acta*. 2006;363(1–2):206–20.
- Wood RC, Luabeya AK, Weigel KM, Wilbur AK, Jones-Engel L, Hatherill M, et al. Detection of *Mycobacterium tuberculosis* DNA on the oral mucosa of tuberculosis patients. *Sci Rep*. 2015;5:8668.
- Parida M, Sannarangaiah S, Dash PK, Rao PV, Morita K. Loop mediated isothermal amplification (LAMP): a new generation of innovative gene amplification technique; perspectives in clinical diagnosis of infectious diseases. *Rev Med Virol*. 2008;18(6):407–21.
- Li Y, Cu YT, Luo D. Multiplexed detection of pathogen DNA with DNA-based fluorescence nanobarcodes. *Nat Biotechnol*. 2005;23(7):885–9.
- Caliendo AM, Gilbert DN, Ginocchio CC, Hanson KE, May L, Quinn TC, et al. Better tests, better care: improved diagnostics for infectious diseases. *Clin Infect Dis*. 2013;57(Suppl 3):S139–70.
- Morgan M, Kalantri S, Flores L, Pai M. A commercial line probe assay for the rapid detection of rifampicin resistance in *Mycobacterium tuberculosis*: a systematic review and meta-analysis. *BMC Infect Dis*. 2005;5:62.
- De Beenhouwer H, Lhiang Z, Jannes G, Mijs W, Machtelinckx L, Rossau R, et al. Rapid detection of rifampicin resistance in sputum and biopsy specimens from tuberculosis patients by PCR and line probe assay. *Tuber Lung Dis*. 1995;76(5):425–30.
- Gautam R, Samuel A, Sil S, Chaturvedi D, Dutta A, Ariese F, Umamathy S. Raman and mid-infrared spectroscopic imaging: applications and advancements. 2015; 108:341–356.
- Kumar S, Matange N, Umamathy S, Visweswariah SS. Linking carbon metabolism to carotenoid production in mycobacteria using Raman spectroscopy. *FEMS Microbiol Lett*. 2015;362(3):1–6.
- Kumar S, Verma T, Mukherjee R, Ariese F, Somasundaram K, Umamathy S. Raman and infra-red microspectroscopy: towards quantitative evaluation for clinical research by ratiometric analysis. *Chem Soc Rev*. 2016;45(7):1879–900.
- Singh B, Gautam R, Kumar S, Kumar BNV, Nongthomba U, Nandi D, et al. Application of vibrational microspectroscopy to biology and medicine. *Curr Sci India*. 2012;102(2):232–44.
- Wang K, Pu H, Sun DW. Emerging spectroscopic and spectral imaging techniques for the rapid detection of microorganisms: an overview. *Compr Rev Food Sci Food Saf*. 2018;17(2):256–73.
- Gautam R, Vanga S, Ariese F, Umamathy S. Review of multidimensional data processing approaches for Raman and infrared spectroscopy. *EPJ Tech Instrum*. 2015;2(1):8.
- Lorenz B, Wichmann C, Stöckel S, Rösch P, Popp J. Cultivation-free Raman spectroscopic investigations of bacteria. *Trends Microbiol*. 2017;25(5):413–24.
- Butler HJ, Ashton L, Bird B, Cinque G, Curtis K, Dorney J, et al. Using Raman spectroscopy to characterize biological materials. *Nat Protoc*. 2016;11:664.
- Kerr LT, Byrne HJ, Hennesly BM. Optimal choice of sample substrate and laser wavelength for Raman spectroscopic analysis of biological specimen. *Anal Methods*. 2015;7(12):5041–52.

19. Eichorst SA, Stasser F, Woyke T, Schintlmeister A, Wagner M, Woebken D. Advancements in the application of NanoSIMS and Raman microspectroscopy to investigate the activity of microbial cells in soils. *FEMS Microbiol Ecol.* 2015;91(10):1–14.
20. McCreery RL. Raman spectroscopy for chemical analysis. USA: Wiley-Interscience Publication; 2001.
21. Read DS, Whiteley AS. Chemical fixation methods for Raman spectroscopy-based analysis of bacteria. *J Microbiol Methods.* 2015;109:79–83.
22. Kloß S, Lorenz B, Dees S, Labugger I, Rösch P, Popp J. Destruction-free procedure for the isolation of bacteria from sputum samples for Raman spectroscopic analysis. *Anal Bioanal Chem.* 2015;407(27):8333–41.
23. Lu X, Al-Qadiri HM, Lin M, Rasco BA. Application of mid-infrared and Raman spectroscopy to the study of bacteria. *Food Bioprocess Technol.* 2011;4(6):919–35.
24. Tang M, McEwen GD, Wu Y, Miller CD, Zhou A. Characterization and analysis of mycobacteria and Gram-negative bacteria and co-culture mixtures by Raman microspectroscopy, FTIR, and atomic force microscopy. *Anal Bioanal Chem.* 2013;405(5):1577–91.
25. Buijtelts PC, Willemse-Erix HF, Petit PL, Endtz HP, Puppels GJ, Verbrugh HA, et al. Rapid identification of mycobacteria by Raman spectroscopy. *J Clin Microbiol.* 2008;46(3):961–5.
26. Maquelin K, Kirschner C, Choo-Smith LP, Ngo-Thi NA, van Vreeswijk T, Stammler M, et al. Prospective study of the performance of vibrational spectroscopies for rapid identification of bacterial and fungal pathogens recovered from blood cultures. *J Clin Microbiol.* 2003;41(1):324–9.
27. Choo-Smith LP, Maquelin K, van Vreeswijk T, Bruining HA, Puppels GJ, Ngo Thi NA, et al. Investigating microbial (micro)colony heterogeneity by vibrational spectroscopy. *Appl Environ Microbiol.* 2001;67(4):1461–9.
28. Rosch P, Harz M, Schmitt M, Peschke KD, Ronneberger O, Burkhardt H, et al. Chemotaxonomic identification of single bacteria by micro-Raman spectroscopy: application to clean-room-relevant biological contaminations. *Appl Environ Microbiol.* 2005;71(3):1626–37.
29. Huang WE, Griffiths RI, Thompson IP, Bailey MJ, Whiteley AS. Raman microscopic analysis of single microbial cells. *Anal Chem.* 2004;76(15):4452–8.
30. Stockel S, Meisel S, Elschner M, Rosch P, Popp J. Identification of *Bacillus anthracis* via Raman spectroscopy and chemometric approaches. *Anal Chem.* 2012;84(22):9873–80.
31. Kloss S, Kampe B, Sachse S, Rosch P, Straube E, Pfister W, et al. Culture independent Raman spectroscopic identification of urinary tract infection pathogens: a proof of principle study. *Anal Chem.* 2013;85(20):9610–6.
32. Kusic D, Kampe B, Rosch P, Popp J. Identification of water pathogens by Raman microspectroscopy. *Water Res.* 2014;48:179–89.
33. Silge A, Schumacher W, Rosch P, Da Costa Filho PA, Gerard C, Popp J. Identification of water-conditioned *Pseudomonas aeruginosa* by Raman microspectroscopy on a single cell level. *Syst Appl Microbiol.* 2014;37(5):360–7.
34. Meisel S, Stockel S, Rosch P, Popp J. Identification of meat-associated pathogens via Raman microspectroscopy. *Food Microbiol.* 2014;38:36–43.
35. Strola SA, Baritoux JC, Schultz E, Simon AC, Al-lie C, Espagnon I, et al. Single bacteria identification by Raman spectroscopy. *J Biomed Opt.* 2014;19(11):111610.
36. Stöckel S, Kirchhoff J, Neugebauer U, Rösch P, Popp J. The application of Raman spectroscopy for the detection and identification of microorganisms. *J Raman Spectrosc.* 2015;47(1):89–109.
37. Baritoux JC, Simon AC, Schultz E, Emain C, Laurent P, Dinten JM. A study on identification of bacteria in environmental samples using single-cell Raman spectroscopy: feasibility and reference libraries. *Environ Sci Pollut Res Int.* 2016;23(9):8184–91.
38. Stockel S, Meisel S, Lorenz B, Kloss S, Henk S, Dees S, et al. Raman spectroscopic identification of *Mycobacterium tuberculosis*. *J Biophotonics.* 2017;10(5):727–34.
39. Munchberg U, Rosch P, Bauer M, Popp J. Raman spectroscopic identification of single bacterial cells under antibiotic influence. *Anal Bioanal Chem.* 2014;406(13):3041–50.
40. Hlaing MM, Wood BR, McNaughton D, Rood JI, Fox EM, Augustin MA. Vibrational spectroscopy combined with transcriptomic analysis for investigation of bacterial responses towards acid stress. *Appl Microbiol Biotechnol.* 2018;102(1):333–43.
41. Neugebauer U, Rosch P, Popp J. Raman spectroscopy towards clinical application: drug monitoring and pathogen identification. *Int J Antimicrob Agents.* 2015;46(Suppl 1):S35–9.
42. Teng L, Wang X, Wang X, Gou H, Ren L, Wang T, et al. Label-free, rapid and quantitative phenotyping of stress response in *E. coli* via ramanome. *Sci Rep.* 2016;6:34359.
43. Kirchhoff J, Glaser U, Bohnert JA, Pletz MW, Popp J, Neugebauer U. Simple ciprofloxacin resistance test and determination of minimal inhibitory concentration within 2 h using Raman spectroscopy. *Anal Chem.* 2018;90(3):1811–8.
44. Yang D, Zhou H, Haisch C, Niessner R, Ying Y. Reproducible *E. coli* detection based on label-free SERS and mapping. *Talanta.* 2016;146:457–63.
45. Ivleva NP, Kubryk P, Niessner R. Raman microspectroscopy, surface-enhanced Raman scattering microspectroscopy, and stable-isotope Raman microspectroscopy for biofilm characterization. *Anal Bioanal Chem.* 2017;409(18):4353–75.
46. Mosier-Boss PA. Review on SERS of bacteria. *Biosens-sors (Basel).* 2017, 7(4).
47. Muhlig A, Bocklitz T, Labugger I, Dees S, Henk S, Richter E, et al. LOC-SERS: a promising closed system for the identification of mycobacteria. *Anal Chem.* 2016;88(16):7998–8004.
48. Rivera-Betancourt OE, Karls R, Grosse-Siestrup B, Helms S, Quinn F, Dluhy RA. Identification of mycobacteria based on spectroscopic analyses of mycolic acid profiles. *Analyst.* 2013;138(22):6774–85.
49. Walter A, Marz A, Schumacher W, Rosch P, Popp J. Towards a fast, high specific and reliable discrimination of bacteria on strain level by means of SERS in a microfluidic device. *Lab Chip.* 2011;11(6):1013–21.
50. Liu T-T, Lin Y-H, Hung C-S, Liu T-J, Chen Y, Huang Y-C, et al. A high speed detection platform based on surface-enhanced Raman scattering for monitoring antibiotic-induced chemical changes in bacteria cell wall. *PLoS One.* 2009;4(5):e5470.
51. Galvan DD, Yu Q. Surface-enhanced Raman scattering for rapid detection and characterization of antibiotic-resistant bacteria. *Adv Healthc Mater.* 2018.
52. Grosse C, Bergner N, Dellith J, Heller R, Bauer M, Mellmann A, et al. Label-free imaging and spectroscopic analysis of intracellular infections. *Anal Chem.* 2015;87(4):2137–42.
53. Silge A, Abdou E, Schneider K, Meisel S, Bocklitz T, Lu-Walther HW, et al. Shedding light on host niches: label-free in situ detection of *Mycobacterium gordonae* via carotenoids in macrophages by Raman microspectroscopy. *Cell Microbiol.* 2015;17(6):832–42.
54. Li R, Goswami U, King M, Chen J, Cesario TC, Rentzepis PM. In situ detection of live-to-dead bacteria ratio after inactivation by means of synchronous fluorescence and PCA. *Proc Natl Acad Sci U S A.* 2018;115(4):668–73.

55. Liu Y, Zhou H, Hu Z, Yu G, Yang D, Zhao J. Label and label-free based surface-enhanced Raman scattering for pathogen bacteria detection: a review. *Biosens Bioelectron.* 2017;94:131–40.
56. Stockel S, Schumacher W, Meisel S, Elschner M, Rosch P, Popp J. Raman spectroscopy-compatible inactivation method for pathogenic endospores. *Appl Environ Microbiol.* 2010;76(9):2895–907.
57. Ramamurthy T, Ghosh A, Pazhani GP, Shinoda S. Current perspectives on viable but non-culturable (VBNC) pathogenic bacteria. *Front Public Health.* 2014;2:103.

Publisher's note Springer Nature remains neutral with regard to jurisdictional claims in published maps and institutional affiliations.